



Infrared multiple photon dissociation spectroscopy of cationized cysteine: Effects of metal cation size on gas-phase conformation

Murat Citir^a, Elana M.S. Stennett^a, Jos Oomens^{b,c}, Jeffrey D. Steill^b, M.T. Rodgers^d, P.B. Armentrout^{a,*}

^a Department of Chemistry, University of Utah, Salt Lake City, UT 84112, United States

^b FOM Institute for Plasma Physics "Rijnhuizen", Edisonbaan 14, 3439 MN Nieuwegein, The Netherlands

^c Van 't Hoff Institute for Molecular Sciences, University of Amsterdam, Amsterdam, The Netherlands

^d Department of Chemistry, Wayne State University, Detroit, MI 48202, United States

ARTICLE INFO

Article history:

Received 11 March 2010

Received in revised form 19 April 2010

Accepted 19 April 2010

Available online 26 April 2010

Keywords:

Alkali metal cation

Amino acid

Conformation

Cysteine

IRMPD

ABSTRACT

The gas-phase structures of cationized cysteine (Cys) including complexes with Li⁺, Na⁺, K⁺, Rb⁺, and Cs⁺, as well as protonated Cys, are examined by infrared multiple photon dissociation (IRMPD) action spectroscopy utilizing light generated by a free electron laser, in conjunction with quantum-chemical calculations. To identify the structures present in the experimental studies, measured IRMPD spectra are compared to spectra calculated at B3LYP/6-311G(d,p) (H⁺, Li⁺, Na⁺, and K⁺ complexes) and B3LYP/HW*/6-311G(d,p) (Rb⁺ and Cs⁺ complexes) levels of theory, where HW* indicates that the Hay-Wadt effective core potential was used on the metals. On the basis of these experiments and calculations, the only conformation that reproduces the IRMPD action spectra for the complexes of the smaller alkali metal cations, Li⁺(Cys) and Na⁺(Cys), is a charge-solvated, tridentate structure where the metal cation binds to the amine and carbonyl groups of the amino acid backbone and the sulfur atom of the side chain, [N,CO,S], in agreement with the predicted ground states of these complexes. For the larger alkali metal cation complexes, K⁺(Cys), Rb⁺(Cys), and Cs⁺(Cys), the spectra have very similar spectral features that are considerably more complex than the IRMPD spectra of Li⁺(Cys) and Na⁺(Cys). For these complexes, the bidentate [COOH] conformer, in which the metal cation binds to both oxygens of the carboxylic acid group, is a dominant contributor, although features associated with the tridentate [N,CO,S] conformer remain and those for the zwitterionic [CO₂⁻] conformer are also clearly present. Theoretical results for Rb⁺(Cys) and Cs⁺(Cys) indicate that both [COOH] and [N,CO,S] conformers are low-energy structures. For H⁺(Cys), the IRMPD action spectrum is reproduced by [N,CO] conformers, in which the protonated amine group hydrogen bonds to the carbonyl oxygen atom and the sulfur atom of the amino acid side chain. Several low-energy [N,CO] conformers that differ only in their side-chain orientations are found and therefore have very similar predicted spectra.

© 2010 Elsevier B.V. All rights reserved.

1. Introduction

Interactions of metal ions with Cys have direct biological significance, but generally involve multiply charged metal cations of Fe, Co, Zn, and Cd [1–8]. A quantitative understanding of the affinity of the sulfur side chain for alkali cations can therefore be useful in examining competition for binding at protein sites involving Cys between these trace metals and the more common alkali metal cations. Recently, the pairwise interactions between Cys and the alkali metal cations, Li⁺, Na⁺, K⁺ and Rb⁺ have been investigated using guided ion beam mass spectrometry [9]. Quantitative bond dissociation energies were determined by threshold

collision-induced dissociation (TCID) and found to be consistent with theoretical values predicted for the ground state (GS) conformations. For Li⁺(Cys) and Na⁺(Cys), charge-solvated tridentate structures that involve binding of the metal cation to the amine and carbonyl groups of the amino acid backbone and the side chain sulfur atom, [N,CO,S] (see nomenclature below), are the ground states and lie well below (>7 kJ/mol) any other conformation, such that quantitative measurements are sufficient to determine the identity of the complexes formed experimentally [9]. Calculations indicate that the energy differences between the ground state and higher energy conformations decrease as the metal cation becomes heavier, Fig. 1. As such, TCID measurements are unable to distinguish between small differences in conformational energy.

In order to assign ground state conformations of these and related complexes more definitively, the present study involves the measurement of IRMPD action spectra for dissociation of Cys

* Corresponding author. Tel.: +1 801 581 7885; fax: +1 801 581 8433.

E-mail address: armentrout@chem.utah.edu (P.B. Armentrout).

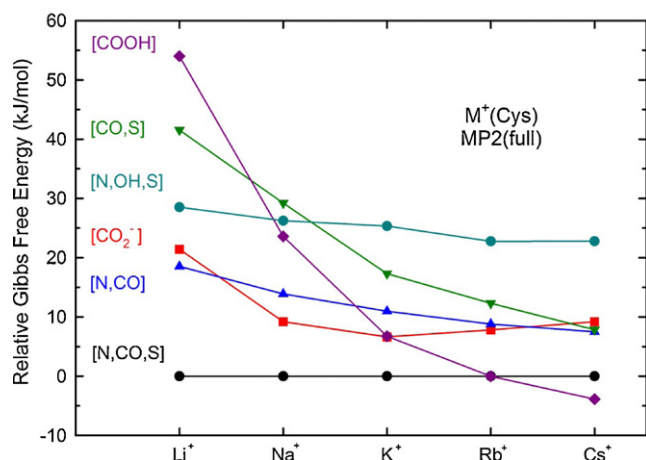


Fig. 1. 298 K Gibbs free energies (kJ/mol) calculated at the MP2(full)/6-311+G(2d,2p)//B3LYP/6-311G(d,p) level of theory for six conformations of $M^+(\text{Cys})$, where $M^+ = \text{Li}^+, \text{Na}^+, \text{K}^+, \text{Rb}^+, \text{and Cs}^+$, as a function of the alkali metal cation relative to the energy of the $[\text{N},\text{CO},\text{S}]$ conformer.

cationized by $\text{H}^+, \text{Li}^+, \text{Na}^+, \text{K}^+, \text{Rb}^+$, and Cs^+ . Infrared multiple photon dissociation (IRMPD) action spectroscopy can be used more directly to examine the presence of specific conformations. Previously sodiated Gly and proline (Pro) [10], and metallated tryptophan (Trp) [11], arginine (Arg) [12], serine (Ser) [13], threonine (Thr) [14], aspartic and glutamic acid (Asp, Glu) [15], asparagine (Asn) [16], and methionine (Met) [17] have been studied by using IRMPD spectroscopy. Here, the conformations are identified by comparing the experimental action spectra to IR spectra derived from quantum-chemical calculations at the B3LYP/6-311G(d,p) level of theory of the low-lying structures of the cationized Cys complexes.

2. Experimental and computational

2.1. Mass spectrometry and photodissociation

Experiments were performed by using a home-built 4.7 T Fourier-transform ion cyclotron resonance (FTICR) mass spectrometer. The instrument has been described in detail elsewhere [18–20]. Tunable radiation for the photodissociation experiments is generated by the free electron laser for infrared experiments (FELIX) [21]. For the present experiments, spectra were recorded over the wavelength range 19.4 μm (520 cm^{-1}) to 5.5 μm (1820 cm^{-1}), which can be covered with a single setting of the electron beam energy of FELIX. Pulse energies were around 50 mJ per macropulse of 5 μs duration, although they fell off to about 20 mJ toward the blue edge of the scan range. Complexes were irradiated for 2–4 s, corresponding to interaction with 10–20 macropulses. The fwhm bandwidth of the laser was typically 0.5% of the central wavelength. The metal cation–cysteine complexes were generated by electrospray ionization using a Micromass Z-Spray source. Solutions of 1.0–3.0 mM Cys with 0.5–1.0 mM alkali-metal chloride (or 1 mM acetic acid for $\text{H}^+(\text{Cys})$) were made up in 50% MeOH and 50% H_2O solutions. Solution flow rates ranged from 10 to 30 $\mu\text{L}/\text{min}$ and the electrospray needle was generally held at a voltage of ~ 3.2 kV. Ions were accumulated in a hexapole trap for about 4 s prior to being injected into the ICR cell via an rf octopole ion guide. Electrostatic pulsing of the dc bias of the ion transfer octopole allows ions to be captured in the ICR cell without the use of a gas pulse [19]. The dc bias switch of the octopole results in there being no change in the dc electric field along the axis of the ion guide which decelerates the ions exiting the octopole. In contrast to the conventional gas pulsing method to stop the ions, this technique does not cause collisional heating of the ions.

2.2. Computational details

In previous work, Armentrout et al. [9] examined likely conformers for cysteine and its alkali cation complexes. The 22–24 low-energy structures were geometry optimized using density functional theory (DFT) at the B3LYP/6-311G(d,p) level [22,23]. Rb^+ and Cs^+ were described using the effective core potentials (ECPs) and valence basis sets of Hay and Wadt [24] with a single d polarization function (exponents of 0.24 and 0.19, respectively) added [25]. This level of theory has been shown to provide a reasonable structural description of comparable metal cation–ligand systems [13,14,16,17]. Relative energies of various conformers were determined from single point energy calculations carried out at the B3LYP, B3P86, and MP2(full) levels using the 6-311+G(2d,2p) and HW* basis sets [22]. Zero-point vibrational energy (ZPE) corrections were determined using vibrational frequencies calculated at the B3LYP/6-311G(d,p) level scaled by a factor of 0.9804 [26]. In the present work, similar procedures were used to identify the low-lying structures of $\text{H}^+(\text{Cys})$ conformers with geometries and vibrational frequencies calculated at the B3LYP/6-311G(d,p) level, followed by single point energy calculations at the same levels as noted above.

Relative energies at 0 K are converted to 298 K free energies using the rigid rotor/harmonic oscillator approximation with rotational constants and vibrational frequencies calculated at the B3LYP/6-311G(d,p) level. These relative ΔG_{298} values are reported in Table S1 of the Supplementary Data. In general, the relative ΔG_{298} excitation energies are comparable to the analogous differences in the ΔH_0 values reported previously [9], although the free energies of the $[\text{N},\text{CO},\text{S}]$ conformers generally increase by several kJ/mol relative to the other conformers because the tridentate binding restricts the flexibility of the complex to a greater extent.

Vibrational frequencies and intensities were calculated using the harmonic oscillator approximation and analytical derivatives of the energy-minimized Hessian calculated at the levels of theory noted above. For comparison to IRMPD spectra, frequencies were scaled by 0.975 as this scaling factor leads to good agreement between calculated and experimentally well-resolved peaks and is in accord with previous IRMPD studies as well [11,16,17]. Calculated vibrational frequencies are broadened using a 20 cm^{-1} fwhm Gaussian line shape for comparison with experimental spectra.

3. Results and discussion

3.1. IRMPD action spectroscopy

Photodissociation spectra of Cys complexed with $\text{Li}^+, \text{Na}^+, \text{K}^+, \text{Rb}^+, \text{Cs}^+$, and H^+ were examined. For metallated Cys complexes with K^+, Rb^+ , and Cs^+ , photodissociation results in the loss of the intact ligand to form the atomic metal cation. This result is consistent with the observation of intact ligand loss as the sole pathway observed in the CID spectra of $\text{K}^+(\text{Cys})$ and $\text{Rb}^+(\text{Cys})$ [9]. In contrast, $\text{Li}^+(\text{Cys})$, $\text{Na}^+(\text{Cys})$, and $\text{H}^+(\text{Cys})$ display alternative decomposition pathways in the IRMPD spectra. For $\text{Li}^+(\text{Cys})$, the CID spectra exhibit three channels corresponding to the loss of the intact amino acid (Cys), NH_3 , and $\text{C}_3\text{H}_4\text{O}_2\text{S}$ [9]. At high energies, the dominant dissociation process observed is the loss of the intact amino acid with the other two fragmentation products observed at lower energies. Deamination was the only decay pathway observed in the IRMPD experiments on $\text{Li}^+(\text{Cys})$, although the Li^+ channel is beyond the accessible mass range of the FTICR. On the other hand, both loss of the intact amino acid and deamination were observed in the IRMPD spectrum for $\text{Na}^+(\text{Cys})$, even though the CID spectrum exhibited only the former channel. For $\text{H}^+(\text{Cys})$, only one decomposition pathway corresponding to the loss of $\text{H}_2\text{O} + \text{CO}$ was observed by IRMPD.

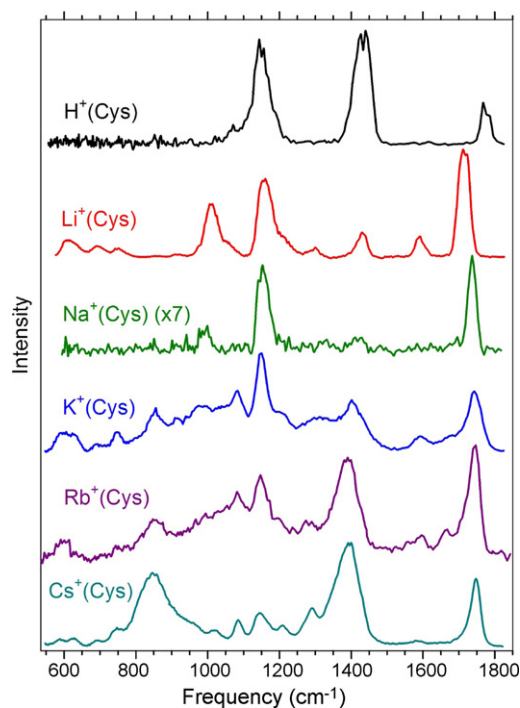


Fig. 2. Infrared multiphoton dissociation action spectra of $M^+(\text{Cys})$ complexes where $M^+ = \text{H}^+, \text{Li}^+, \text{Na}^+, \text{K}^+, \text{Rb}^+, \text{and } \text{Cs}^+$.

For the K^+ , Rb^+ , and Cs^+ complexes of Cys, IRMPD action spectra are taken from the relative intensity of the M^+ product cation as a function of laser wavelength. For the Na^+ and Li^+ complexes of Cys, the sum of all observed reaction pathways is shown. For $\text{H}^+(\text{Cys})$, the decomposition pathway corresponding to the loss of $\text{H}_2\text{O} + \text{CO}$ is shown as the IRMPD action spectrum. The results are shown in Fig. 2. Linear corrections for laser power are applied, which mainly affects the relative intensities observed at the highest laser frequencies.

Comparison of the IRMPD spectra in Fig. 2 shows that the features observed in the $\text{Li}^+(\text{Cys})$ spectrum are retained for all of the metal cation complexes, but that new spectral features begin to appear for $\text{K}^+(\text{Cys})$ and become very obvious for $\text{Cs}^+(\text{Cys})$. The major band at 1718 cm^{-1} shifts to the blue and the bands at 1429 , 1299 , and 1160 cm^{-1} shift to the red as the metal cation becomes heavier. The band at 1429 cm^{-1} for $\text{Li}^+(\text{Cys})$ red shifts to 1401 cm^{-1} in $\text{K}^+(\text{Cys})$, and the photodissociation signal in this frequency range increases substantially for $\text{Rb}^+(\text{Cys})$, and $\text{Cs}^+(\text{Cys})$. A spectral feature at 1592 cm^{-1} remains largely unchanged as the size of the metal ion increases. A new band emerges at 1684 cm^{-1} for $\text{K}^+(\text{Cys})$ and at 1667 cm^{-1} for $\text{Rb}^+(\text{Cys})$, but is less distinct for $\text{Cs}^+(\text{Cys})$. These progressions suggest multiple conformers are now present in the IRMPD spectra for the K^+ , Rb^+ , and Cs^+ complexes.

3.2. Theoretical results (structures)

A detailed discussion of the structures of cysteine and its metal cation complexes with Li^+ , Na^+ , K^+ , Rb^+ , and Cs^+ can be found elsewhere [9]. Low-lying and representative higher energy conformations of $\text{Cs}^+(\text{Cys})$ are shown in Fig. 3 and S1, respectively. The nomenclature used to identify these different structural isomers is based on that established previously for $M^+(\text{Gly})$ [27–30]. Briefly, conformations of cationized Cys are identified by their metal binding sites in brackets, followed by a description of the cysteine orientation, named by the series of dihedral angles starting from the carboxylic acid hydrogen of the backbone (or the analogous proton on NH_2 in zwitterionic structures) and going to the terminal

Table 1

Relative enthalpies at 0 K and free energies at 298 K (kJ/mol) of low-lying conformers of $\text{H}^+(\text{Cys})^a$.

Structure	B3LYP	B3P86	MP2(full)
[N,CO]-tggg ₊	0.0 (0.0)	0.0 (0.0)	0.0 (0.0)
[N,CO]-tgtg ₊	0.3 (−0.1)	1.4 (1.0)	1.9 (1.6)
[N,CO]-tggg _−	4.5 (3.8)	4.5 (3.9)	5.4 (4.8)
[N,CO]-tgtg _−	4.4 (3.3)	5.6 (4.5)	6.6 (5.5)

^a Free energies in parentheses. All values calculated at the level of theory indicated using the 6-311+G(2d,2p) basis set with structures and zero-point energies calculated at the B3LYP/6-311G(d,p) level of theory.

side-chain sulfur ($\angle\text{HOCC}$, $\angle\text{OCCC}$, $\angle\text{CCCS}$, and $\angle\text{CCSH}$, respectively). The dihedral angles are distinguished as cis (c, for angles between 0° and 45°), gauche (g, 45° and 135°), or trans (t, 135° and 180°). The zwitterionic conformer is designated as $[\text{CO}_2^-]$.

Relative energies at 0 K including ZPE corrections with respect to the ground state calculated at three different levels of theory (B3LYP, B3P86, and MP2(full)) can be found elsewhere for $M^+(\text{Cys})$ complexes, where $M^+ = \text{Li}^+, \text{Na}^+, \text{K}^+, \text{Rb}^+, \text{and } \text{Cs}^+$ [9]. The relative Gibbs free energies at 298 K may be more relevant in describing the experimental distributions investigated here and these are provided in Table S1. The overall trends in relative Gibbs free energies at 298 K calculated at the MP2(full) level are shown in Fig. 1. These results are qualitatively similar to those calculated at the B3LYP and B3P86 levels, for which figures can be found in Supplementary Data, Fig. S2.

At nearly all levels of theory, the ground state structure for $\text{Li}^+(\text{Cys})$, $\text{Na}^+(\text{Cys})$, and $\text{K}^+(\text{Cys})$ is the [N,CO,S]-tggg conformer, a tridentate charge-solvated structure in which the metal ion binds to the backbone amino nitrogen, backbone carbonyl oxygen, and the side-chain sulfur. There are two variants of this structure, tggg₊ and tggg_−, which differ only in whether the SH bond points in the same direction as the carboxylic acid group or the amino group, respectively, Figs. 3 and S1. According to the DFT results, the ground state structures for $\text{Rb}^+(\text{Cys})$ and $\text{Cs}^+(\text{Cys})$ are bidentate [COOH] geometries in which the metal cation binds to both oxygens of the carboxylic acid group and there is an $\text{OH} \cdots \text{N}$ hydrogen bond (Fig. 3). For $\text{Rb}^+(\text{Cys})$, the [N,CO,S]-tggg₊ structure is the ground state at the MP2(full) level of theory and is 2.4–5 kJ/mol above the ground state at the two DFT levels of theory (5–8 kJ/mol in 298 K free energy), whereas for $\text{Cs}^+(\text{Cys})$, calculations indicate that [COOH]-ctg_−g_− is still the ground state structure. Closely related structures are the zwitterionic $[\text{CO}_2^-]$ complexes in which the metal cation interacts with both oxygens of the carboxylate moiety (Fig. 3). These zwitterions differ from [COOH] structures primarily in the slight change in the position of the proton shared by the carboxylic and amino groups. A somewhat higher energy structure is bidentate [N,CO], in which the metal cation binds to the backbone amino nitrogen and backbone carbonyl oxygen (Fig. S1). At still higher energies, there are [N,OH,S] and [CO,S] structures (Fig. S1). The latter three structures remain at elevated energies for all alkali metal cations (Fig. 1).

Lastly, the protonated cysteine complex, $\text{H}^+(\text{Cys})$, has a set of low-energy structures, [N,CO], in which the protonated amine group hydrogen bonds to both the carbonyl oxygen atom ($\text{NH} \cdots \text{OC}$) and the sulfur atom of the amino acid side chain ($\text{NH} \cdots \text{S}$). A third hydrogen bond is also present between the hydroxyl group and the carbonyl oxygen atom. Four structures having this bonding motif vary in the side-chain orientations: tggg₊, tggg_−, tgtg_−, and tgtg₊ (Fig. 3). Single point energies including ZPE corrections calculated at three different levels of theory, relative to the lowest energy isomer, are given in Table 1 for $\text{H}^+(\text{Cys})$, which also lists the relative free energies at 298 K of these conformers. At all levels of theory, the ground state structure for $\text{H}^+(\text{Cys})$ is the [N,CO]-tggg₊ conformer.

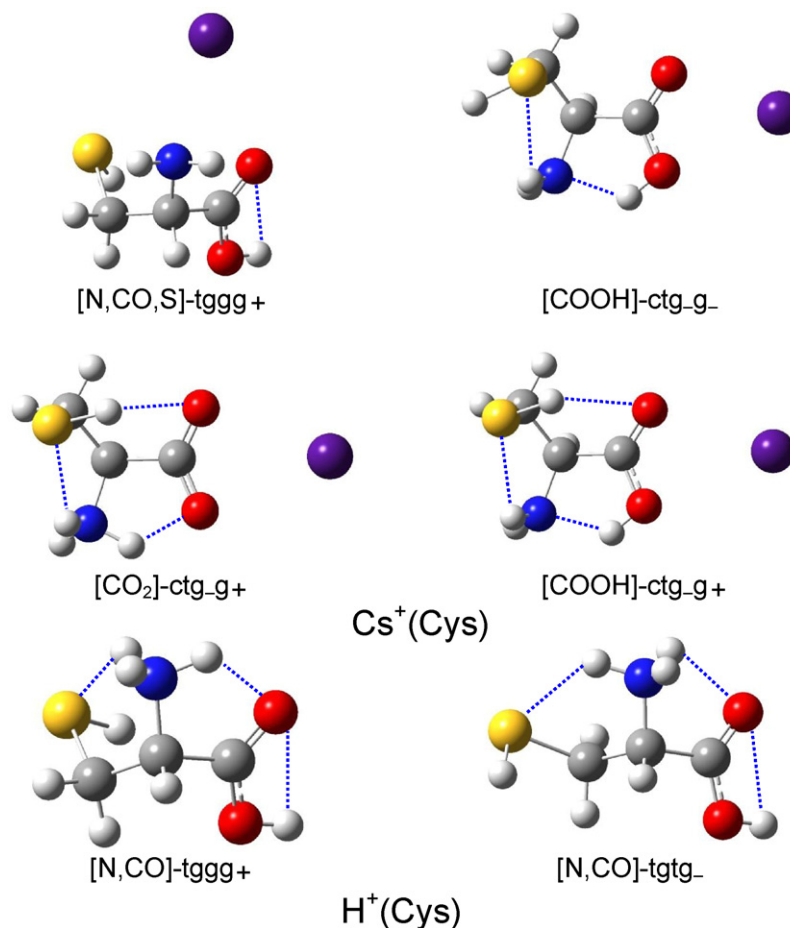


Fig. 3. Structures of the $\text{Cs}^+(\text{Cys})$ and $\text{H}^+(\text{Cys})$ complexes calculated at the B3LYP/HW*/6-311G(d,p) level of theory. Dashed lines indicate hydrogen bonds.

3.3. Comparison of experimental and theoretical IR spectra: $\text{Li}^+(\text{Cys})$

Fig. 4 compares the experimental IRMPD action spectrum with calculated IR spectra for three distinct conformers of $\text{Li}^+(\text{Cys})$. The calculated IR intensities may not be in direct accordance with the IRMPD action spectrum because the latter is a multiple photon process, whereas the theoretical IR spectra are based on single photon absorption. Nevertheless, the bands predicted by the $[\text{N},\text{CO},\text{S}]\text{-tggg}_+$ conformer correspond well with the observed spectrum, in terms of both band positions and relative intensities. The alternative side-chain orientation, $[\text{N},\text{CO},\text{S}]\text{-tggg}_-$ is sufficiently low in energy (~ 3 kJ/mol) that it could also contribute to the experimental spectrum, but its predicted spectral features are essentially identical to those of the tggg_- conformer. The calculated IR spectra and frequencies for higher energy structures are included in the Supplementary Data (Fig. S3 and Tables S1–S7), but none of these are predicted to be low enough in energy to contribute to the experimental spectrum.

The band observed at 1718 cm^{-1} corresponds to the carbonyl stretch, which explains its large intensity. Interaction with the lithium cation results in a red shift of this band with respect to free Cys, calculated at 1799 cm^{-1} for the N2-g_+ type GS conformation [9]. The CO stretch predicted by the $[\text{N},\text{CO},\text{S}]\text{-tggg}_+$ conformer at 1715 cm^{-1} agrees well with the observed band. Similar carbonyl stretches are found in five of the seven distinct conformers of $\text{Li}^+(\text{Cys})$ (Fig. 4 and S3), the exceptions being $[\text{N},\text{OH},\text{S}]\text{-tggg}_+$, $[\text{CO},\text{S}]\text{-tgtg}$, and $[\text{CO}_2]\text{-ctg}_g+$. In the $[\text{N},\text{OH},\text{S}]\text{-tggg}_+$ conformer, the metal cation binds to the hydroxyl group of the backbone rather

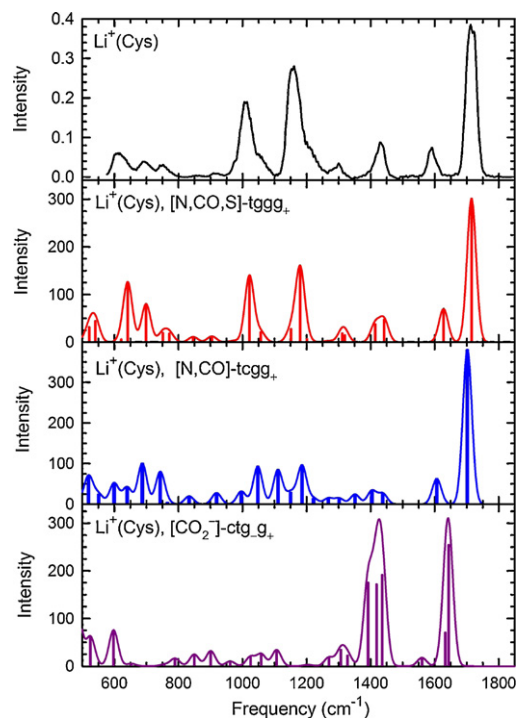


Fig. 4. Comparison of the experimental IRMPD action spectrum for $\text{Li}^+(\text{Cys})$ with IR spectra for three low-lying conformations predicted at the B3LYP/6-311G(d,p) level of theory.

than to the carbonyl, resulting in a blue shift (to 1851 cm^{-1}) of the carboxylic acid CO stretch. For [CO,S]-ttgt, the carboxylic acid CO stretch is red shifted compared to the [CO,S]-ctgt conformer. The difference between the two [CO,S] structures lies in the orientation of the hydrogen bond of the carboxylic acid hydrogen. In [CO,S]-ctgt, this hydrogen interacts with the amino nitrogen, whereas in [CO,S]-ttgt, the H-bond is formed within the carboxylic acid group, leading to the observed red shift. For the zwitterion ($[\text{CO}_2^-]\text{-ctg}_+\text{-g}_+$), the carboxylate functionality is predicted to have a CO stretch that is significantly red shifted to 1642 cm^{-1} (Fig. 4).

The band observed at 1592 cm^{-1} has the largest deviation with the calculated spectra for the [N,CO,S]-tggg₊ conformer, which has a band predicted at 1628 cm^{-1} . This band is associated with the bending motion of the NH_2 group. Such deviations between experiment and theory have been observed for NH_2 bending modes in other systems [13,14,31,32] and are believed to result from strong anharmonic effects.

The bands observed at 1159 and 1011 cm^{-1} are probably the most diagnostic bands for the [N,CO,S]-tggg₊ structure. The position and relative intensity of these bands are nicely reproduced by the predicted IR spectrum for this conformer, whereas no other conformation is predicted to have dominant bands at these same characteristic frequencies. The bands at 1159 and 1011 cm^{-1} are primarily associated with a bending motion of the COH group and the NH_2 wagging motion, with the predicted bands slightly blue shifted by 20 and 11 cm^{-1} , respectively.

Less intense peaks observed at 1429 , 750 , 694 , and 615 cm^{-1} are well represented by the spectra calculated for the [N,CO,S] conformer. The band at 1429 cm^{-1} corresponds to HCH bends in the amino acid side chain. Peaks observed at 750 , 694 , and 615 cm^{-1} correspond to wagging motions of the carboxylic acid hydrogen atom. The very weak bands observed at 1299 , 908 , and 860 cm^{-1} are also consistent with bands predicted in the [N,CO,S] spectrum. Overall, the experimental IRMPD action spectrum can be explained completely by the calculated spectrum of the ground state [N,CO,S] tggg₊ conformer.

3.4. Comparison of experimental and theoretical IR spectra: $\text{Na}^+(\text{Cys})$

As shown in Fig. 2, the IRMPD action spectra for $\text{Na}^+(\text{Cys})$ and $\text{Li}^+(\text{Cys})$ are very similar, exhibiting all of the same major spectral features, although because of the poorer signal to noise level in the $\text{Na}^+(\text{Cys})$ spectrum, some of the weak bands are not evident. Comparison of the experimental and theoretical spectra for $\text{Na}^+(\text{Cys})$ can be found in Fig. S4 of the Supplementary Information. The predicted spectrum for the [N,CO,S]-tggg₊ conformer shows a close correspondence to the observed spectrum for $\text{Na}^+(\text{Cys})$. The intense band observed at 1737 cm^{-1} agrees well with the predicted carbonyl stretch for the lowest energy [N,CO,S]-tggg₊ conformer at 1734 cm^{-1} . The calculated spectra correctly predict a blue shift in this band of 19 cm^{-1} from $\text{Li}^+(\text{Cys})$ to $\text{Na}^+(\text{Cys})$. Likewise the bands at 1011 and 1159 cm^{-1} in the $\text{Li}^+(\text{Cys})$ spectrum are red shifted for $\text{Na}^+(\text{Cys})$ to 993 and 1154 cm^{-1} (shifts of 18 and 5 cm^{-1}), respectively, in reasonable agreement with predicted red shifts of 12 and 8 cm^{-1} for [N,CO,S]-tggg₊. In addition, weak bands observed in the $\text{Na}^+(\text{Cys})$ spectrum at 1328 and 1420 cm^{-1} are reproduced in the predicted spectrum for [N,CO,S]-tggg₊. The former band is blue-shifted by 29 cm^{-1} from $\text{Li}^+(\text{Cys})$ to $\text{Na}^+(\text{Cys})$, whereas the latter band is red shifted by 9 cm^{-1} , consistent with theoretical predictions. Predicted bands in the region of $550\text{--}950$ are not evident in the $\text{Na}^+(\text{Cys})$ spectrum. Despite the limited signal to noise, the predicted spectra for the [N,CO,S] conformers of $\text{Li}^+(\text{Cys})$ and $\text{Na}^+(\text{Cys})$ accurately represent the changes observed with metal cation identity.

3.5. Comparison of experimental and theoretical IR spectra: $\text{K}^+(\text{Cys})$ and $\text{Rb}^+(\text{Cys})$

Compared to the experimental spectra for $\text{Li}^+(\text{Cys})$ and $\text{Na}^+(\text{Cys})$, the IRMPD spectrum of $\text{K}^+(\text{Cys})$ retains all the same bands, but new features are present, see Fig. 2. The spectrum for $\text{Rb}^+(\text{Cys})$ is very similar to that for $\text{K}^+(\text{Cys})$, having the same number of new bands compared to the $\text{Li}^+(\text{Cys})$ and $\text{Na}^+(\text{Cys})$ spectra. The appearance of these new bands could be evidence for new conformers or could be the result of better sensitivity associated with more facile dissociation of these more weakly bound systems. New bands in the observed spectrum of $\text{K}^+(\text{Cys})$ [$\text{Rb}^+(\text{Cys})$] occur at 855 [855], 1083 [1082], and 1680 [1668] cm^{-1} . In addition, the band at 1401 [1390] cm^{-1} grows in intensity with respect to $\text{Na}^+(\text{Cys})$ and there is a general increase in intensity in the region between this band and the band at 1150 cm^{-1} with a broad low frequency shoulder. Overall, a comparison between the $\text{K}^+(\text{Cys})$ and $\text{Rb}^+(\text{Cys})$ spectra with those of $\text{Li}^+(\text{Cys})$ and $\text{Na}^+(\text{Cys})$ shows a considerable increase in photodissociation in the region from 700 to 1500 cm^{-1} .

Fig. 5 shows the experimental IRMPD action spectrum of $\text{K}^+(\text{Cys})$ compared with theoretical predictions for the seven lowest energy distinct conformations (those having different metal cation binding modes). Comparison of the experimental and theoretical spectra for $\text{Rb}^+(\text{Cys})$ can be found in the Supplementary Data, Fig. S5. The overall results for $\text{Rb}^+(\text{Cys})$ are very similar to those shown for $\text{K}^+(\text{Cys})$. The [N,CO,S] conformer may still be present as the predicted carbonyl stretch of 1744 [1756] cm^{-1} agrees well with the corresponding band observed at 1743 [1747] cm^{-1} . The frequency for the bending mode of the NH_2 group in the [N,CO,S] spectra (1624 [1626] cm^{-1}) is blue shifted by $\sim 30\text{ cm}^{-1}$ with respect to the observed band at 1593 [1596] cm^{-1} , consistent with the observed shifts for $\text{Li}^+(\text{Cys})$ and $\text{Na}^+(\text{Cys})$. The calculated band at 1158 [1152] cm^{-1} corresponding to the COH bending mode of the [N,CO,S] conformer matches the observed spectrum for $\text{K}^+(\text{Cys})$ [$\text{Rb}^+(\text{Cys})$] well (1150 [1147] cm^{-1}). This band is particularly diagnostic for the presence of the [N,CO,S] conformer as only this conformer and the higher energy [N,CO]-tggg₊ and [CO,S]-ttgt conformers show an intense band at this frequency. Likewise, the wagging motions of the carboxylic acid hydrogen atom below 800 cm^{-1} in the observed $\text{K}^+(\text{Cys})$ [$\text{Rb}^+(\text{Cys})$] spectrum are also well characterized in the calculated spectrum for the [N,CO,S] conformer. Bands observed at ~ 974 [~ 994], and 1083 [1082] cm^{-1} could also have contributions from the [N,CO,S] conformer.

The [COOH]-ctg₋g₋ conformer must also be considered as it is predicted to be low in energy, $4\text{--}11\text{ kJ/mol}$ ($0\text{--}7\text{ kJ/mol}$ in 298 K free energy) higher than the [N,CO,S]-tggg₊ conformer for $\text{K}^+(\text{Cys})$ and the ground state structure for $\text{Rb}^+(\text{Cys})$ at the DFT level. The intense band observed at 1743 [1747] cm^{-1} agrees well with the predicted carbonyl stretch for the [COOH]-ctg₋g₋ conformer at 1754 [1766] cm^{-1} , but overlaps directly with the carbonyl stretch in the [N,CO,S] spectrum. However, the bands near 1400 and 1750 cm^{-1} are distinct in their predicted one-photon relative intensities for [N,CO,S] and [COOH]. A mixture of these two structures seems likely to explain the experimentally observed relative intensities in the $\text{K}^+(\text{Cys})$ and $\text{Rb}^+(\text{Cys})$ spectra. The NH_2 bending mode in the [COOH] spectrum (1606 [1607] cm^{-1}) is still blue shifted by 13 [~ 11] cm^{-1} with respect to the observed band at 1593 [~ 1596] cm^{-1} . The new band observed at 855 [855] cm^{-1} is attributed to the NH_2 umbrella (857 [856] cm^{-1}) modes of the [COOH] conformer. The relative intensity of this band as well as those between 900 and 1000 cm^{-1} seems much more consistent with the [COOH] spectrum than [N,CO,S].

The small peak at 1684 cm^{-1} in the observed spectrum for $\text{K}^+(\text{Cys})$ and much more obvious band at 1668 cm^{-1} in the $\text{Rb}^+(\text{Cys})$ spectrum clearly indicate the presence of the zwitterionic $[\text{CO}_2^-]$

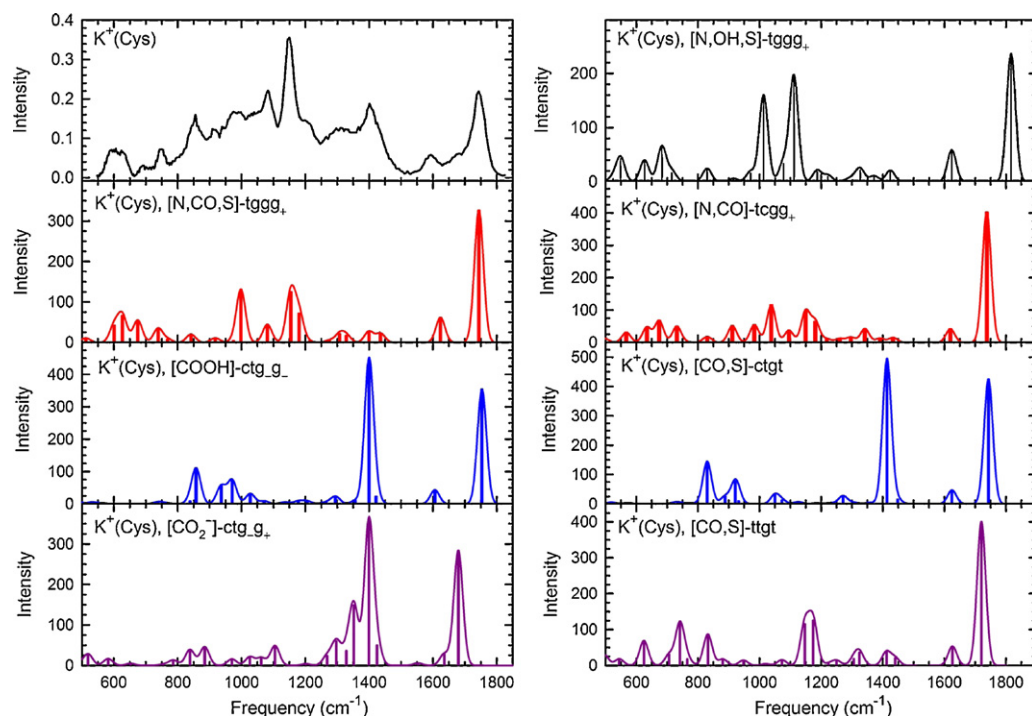


Fig. 5. Comparison of the experimental IRMPD action spectrum for $K^+(Cys)$ with IR spectra for seven low-lying conformations predicted at the B3LYP/6-311G(d,p) level of theory.

conformer. The observed band agrees well with the calculated spectrum (1680 cm^{-1}) for $K^+(Cys)$, whereas that predicted for $Rb^+(Cys)$ (1696 cm^{-1}) is somewhat too high. Further evidence for the $[CO_2^-]$ conformers is the broad shoulder to the red of the band observed at 1401 [1390] cm^{-1} .

Overall, the experimental spectra for $K^+(Cys)$ and $Rb^+(Cys)$ are adequately represented by contributions from the $[N,CO,S]$, $[COOH]$, and $[CO_2^-]$ conformers. This is consistent with calculations for $K^+(Cys)$ and $Rb^+(Cys)$, which indicate that any other conformers lie at least 8 kJ/mol higher in energy[9] (8 kJ/mol higher in 298 K free energy, Table S1), suggesting that they can contribute no more than a few percent to the overall population.

3.6. Comparison of experimental and theoretical IR spectra: $Cs^+(Cys)$

The IRMPD action spectrum of $Cs^+(Cys)$ clearly presents trends consistent with $K^+(Cys)$ and $Rb^+(Cys)$, see Fig. 2. The same bands are present but peaks at 845 , 1294 , and 1392 cm^{-1} increase in relative intensity, whereas those below 700 and between 1000 and 1200 cm^{-1} decrease in relative intensity. Therefore, all of the comparisons between the observed spectrum and the predicted spectra mentioned in the previous section are still viable. Fig. 6 compares the experimental spectrum of $Cs^+(Cys)$ with theoretical predictions for three distinct low-energy conformers.

According to the DFT calculations, the ground state structure for $Cs^+(Cys)$ is the bidentate $[COOH]-ctg_g$ conformer. The $[N,CO,S]$ $tggg_+$ conformer lies 1 (MP2) or 7 – 10 (DFT) kJ/mol above the ground state structure (4 and 10 – 13 kJ/mol higher at 298 K) [9]. The intense band observed at 1745 cm^{-1} agrees well with the predicted carbonyl stretch for the $[COOH]-ctg_g$ and $[N,CO,S]-tggg_+$ conformers at 1753 and 1746 cm^{-1} , respectively. The NH_2 bending mode in the $[COOH]$ and $[N,CO,S]$ spectra (1606 and 1620 cm^{-1}) is still blue shifted by 28 and 42 cm^{-1} with respect to the observed band at 1578 cm^{-1} , consistent with observations for $K^+(Cys)$ and $Rb^+(Cys)$. The diagnostic features observed at 550 – 750 , 1084 , and

1144 cm^{-1} indicate that $[N,CO,S]$ is clearly present. The observed bands at 1392 and 845 cm^{-1} are attributed to the C–O–H bending (1393 cm^{-1}) and NH_2 umbrella (868 cm^{-1}) modes of the $[COOH]$ conformer. The new feature observed for K^+ and Rb^+ complexes around 1670 cm^{-1} is no longer obvious, but probably is associated with the low frequency shoulder on the intense peak at 1745 cm^{-1} .

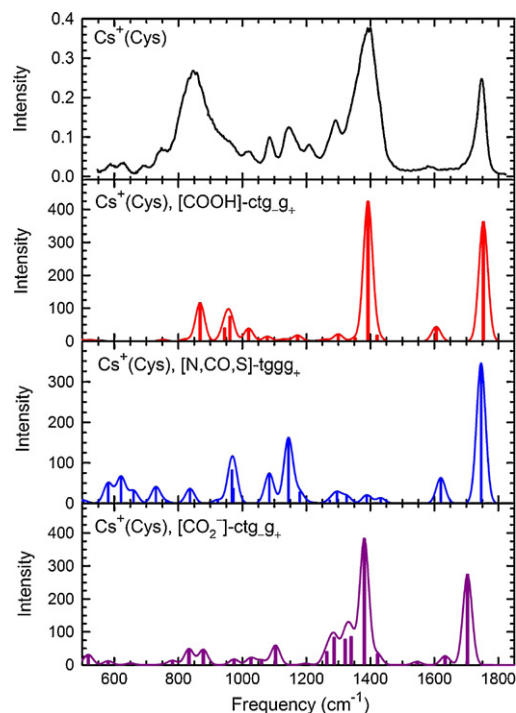


Fig. 6. Comparison of the experimental IRMPD action spectrum for $Cs^+(Cys)$ with IR spectra for three low-lying conformations predicted at the B3LYP/HW*/6-311G(d,p) level of theory.

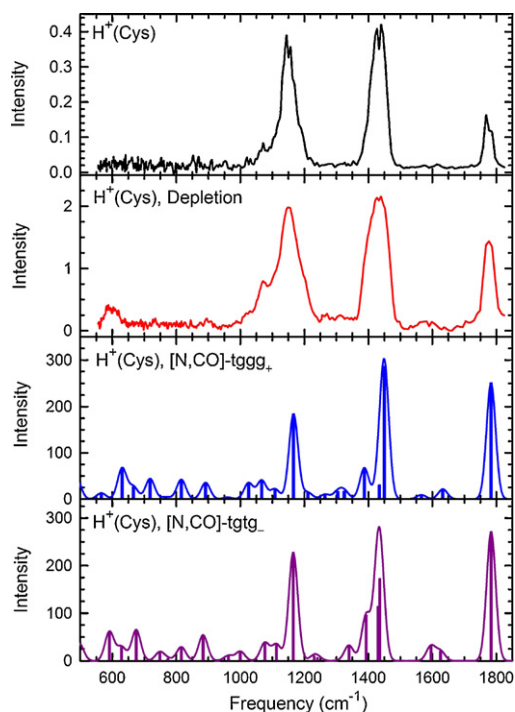


Fig. 7. Comparison of the experimental IRMPD action spectrum for $\text{H}^+(\text{Cys})$ with IR spectra for two low-lying conformations predicted at the B3LYP/6-311G(d,p) level of theory.

This is potentially consistent with calculations for the $[\text{CO}_2^-]$ conformers, which have calculated carbonyl stretches at 1703 cm^{-1} , i.e., the difference between the carbonyl stretches in the $[\text{COOH}]$ and $[\text{CO}_2^-]$ conformers is smaller for the Cs^+ complex ($\sim 50\text{ cm}^{-1}$) than for K^+ and Rb^+ ($\sim 70\text{ cm}^{-1}$). Certainly both of these conformers can contribute to the observed band at 1392 cm^{-1} with predicted frequencies at 1393 cm^{-1} for $[\text{COOH}]$ and 1381 cm^{-1} for $[\text{CO}_2^-]$. The shoulder observed to the red of this band seems indicative of the $[\text{CO}_2^-]$ conformer.

Both $[\text{N,CO,S}]$ and $[\text{COOH}]$ conformers clearly contribute to the observed spectrum for $\text{Cs}^+(\text{Cys})$, but the intensity of the modes associated with $[\text{N,CO,S}]$ are less intense compared to the $\text{K}^+(\text{Cys})$ and $\text{Rb}^+(\text{Cys})$ spectra, consistent with the change in relative energies of these conformers with metal ion, Fig. 1. The presence of the $[\text{CO}_2^-]$ conformer is again possible; however, the peak corresponding to the asymmetric carboxylate stretch is certainly not as clear as for $\text{K}^+(\text{Cys})$ and $\text{Rb}^+(\text{Cys})$. This is also consistent with the relative energy of the zwitterion conformer, which increases for $\text{Cs}^+(\text{Cys})$ in contrast to the trend observed for the lighter metal complexes. This trend is similar to that for other amino acids with functionalized side chains [11–14,16,17], but differs from that for the aliphatic amino acids where the zwitterion reaches its maximum relative stability for sodium cation complexes [33].

3.7. Comparison of experimental and theoretical IR spectra: $\text{H}^+(\text{Cys})$

The IRMPD action spectrum of $\text{H}^+(\text{Cys})$ is unique among the six systems investigated here, as the proton is covalently bound to the amine group. Fig. 7 compares the experimental spectrum of the product ion (loss of $\text{H}_2\text{O} + \text{CO}$) spectrum and the $\text{H}^+(\text{Cys})$ depletion spectrum with those calculated for the two most stable conformers. Only two spectra are shown for the four low-energy $[\text{N,CO}]$ conformations as the calculated IR spectra are identical for tg^+gg^+ and tg^+gg^- orientations and for tgtg^- and tgtg^+ orientations. The experimental spectra exhibit three major peaks at

about 1774 , 1430 , and 1150 cm^{-1} , and additional weak bands are observed in the depletion spectrum at 1578 , 1071 , 895 , 732 , and 598 cm^{-1} . The peak observed at 1774 cm^{-1} corresponds to the carbonyl stretch, whereas the peaks at 1578 and 1430 cm^{-1} correspond to NH_3 bending and umbrella motions, respectively. The 1150 and 598 cm^{-1} bands correspond mostly to COH bending and wagging motions, respectively, of the hydroxyl group. The weak 1071 , 895 , and 732 cm^{-1} bands have a more delocalized character. It can also be noted that predicted bands at about 1250 and 1330 cm^{-1} , which correspond to wagging motions of the alpha carbon hydrogen atom and CH_2 groups of the amino acid side chain, may be consistent with photodissociation intensity observed in the depletion spectrum.

All of these peaks are consistent with the lowest-energy conformers, $[\text{N,CO}]\text{-tg}^+\text{gg}^+_{/-}$ and $[\text{N,CO}]\text{-tgtg}^-_{/+}$. The $\text{H}^+(\text{Cys})$ carbonyl stretch in the observed spectrum (1774 cm^{-1}) is reproduced well by the $[\text{N,CO}]$ spectra ($1783\text{--}1784\text{ cm}^{-1}$). The bending and umbrella motions of the NH_3 group and COH bending motion in the calculated spectrum of the $[\text{N,CO}]\text{-tg}^+\text{gg}^+_{/-}$ conformer for $\text{H}^+(\text{Cys})$ are blue shifted (by $\sim 18\text{ cm}^{-1}$) with respect to the observed peaks at 1430 and 1150 cm^{-1} . The broad peak observed spanning the range from 1350 to 1500 cm^{-1} suggests that a mixture of $[\text{N,CO}]$ structures is most consistent with the observed spectrum. In addition, the shoulder located at frequencies below the 1150 cm^{-1} peak is reproduced by the $\text{tg}^+\text{gg}^+_{/-}$ and $\text{tgtg}^-_{/+}$ calculated spectra, as are the weak bands at 598 , 732 , 895 , and 1578 cm^{-1} .

3.8. Overview

We can now provide a more global comparison of the main features in all six spectra in Fig. 2. The predicted frequencies for the CO stretch of the $[\text{N,CO,S}]\text{-tg}^+\text{gg}^+$ conformer change from 1715 cm^{-1} for $\text{Li}^+(\text{Cys})$ to 1734 cm^{-1} for $\text{Na}^+(\text{Cys})$ to 1744 cm^{-1} for $\text{K}^+(\text{Cys})$ to 1756 cm^{-1} for $\text{Rb}^+(\text{Cys})$ to 1746 cm^{-1} for $\text{Cs}^+(\text{Cys})$, in agreement with the observed blue shift in the experimental spectra from 1718 cm^{-1} for $\text{Li}^+(\text{Cys})$ to 1737 cm^{-1} for $\text{Na}^+(\text{Cys})$ to 1743 cm^{-1} for $\text{K}^+(\text{Cys})$ to 1747 cm^{-1} for $\text{Rb}^+(\text{Cys})$ to 1745 cm^{-1} for $\text{Cs}^+(\text{Cys})$. The CO stretch of the $[\text{COOH}]$ conformers shows a similar shift changing from 1754 cm^{-1} for $\text{K}^+(\text{Cys})$ to 1766 cm^{-1} for $\text{Rb}^+(\text{Cys})$ to 1753 cm^{-1} for $\text{Cs}^+(\text{Cys})$. These blue shifts result from decreased perturbations on the CO stretches as the metal cation binding strength decreases. The observed band at 1159 cm^{-1} in the $\text{Li}^+(\text{Cys})$ spectrum red shifts to 1144 cm^{-1} for $\text{Cs}^+(\text{Cys})$. This shift is consistent with that predicted for the COH bending motion of $[\text{N,CO,S}]\text{-tg}^+\text{gg}^+$ conformers with predicted frequencies of 1179 cm^{-1} for $\text{Li}^+(\text{Cys})$, 1171 cm^{-1} for $\text{Na}^+(\text{Cys})$, 1158 cm^{-1} for $\text{K}^+(\text{Cys})$, 1152 cm^{-1} for $\text{Rb}^+(\text{Cys})$, and 1144 cm^{-1} for $\text{Cs}^+(\text{Cys})$. The observed band at about 1592 cm^{-1} in all of the spectra is not accurately predicted because of the anharmonicity in the bending motion of the NH_2 group. This band does not shift with metal cation identity, in agreement with the predictions for the $[\text{N,CO,S}]\text{-tg}^+\text{gg}^+$ conformers.

Prominent new peaks emerging at 855 cm^{-1} for $\text{K}^+(\text{Cys})$, 855 cm^{-1} for $\text{Rb}^+(\text{Cys})$, and 845 cm^{-1} for $\text{Cs}^+(\text{Cys})$ are diagnostic for the presence of the $[\text{COOH}]$ conformer. Likewise, the CO stretch of the $[\text{CO}_2^-]$ conformers first appears in the IRMPD action spectrum for $\text{K}^+(\text{Cys})$ at 1684 cm^{-1} and red shifts to 1668 cm^{-1} for $\text{Rb}^+(\text{Cys})$. This band is not as well defined for $\text{Cs}^+(\text{Cys})$, which is consistent with the increasing relative energy of the zwitterionic conformer compared to the charge-solvated $[\text{COOH}]$ species as the metal ion gets heavier (Fig. 1).

Bands near 1400 cm^{-1} are observed in all of the spectra shown in Fig. 2, but are also common to the predicted spectra of the $[\text{N,CO,S}]$, $[\text{COOH}]$, and $[\text{CO}_2^-]$ conformers. The band observed at 1429 cm^{-1} in the $\text{Li}^+(\text{Cys})$ spectrum red shifts to 1392 cm^{-1} for $\text{Cs}^+(\text{Cys})$ and becomes more intense. This shift is consistent with that pre-

dicted for the COH bending motion of [N,CO,S]-tggg⁺ conformers with predicted frequencies of 1436, 1408–1428, 1401, 1395, and 1389 cm⁻¹ for Li⁺(Cys)–Cs⁺(Cys), respectively. In contrast, the predicted frequencies for the COH bending motion of the [COOH] conformers generally blue shift, changing from 1381 cm⁻¹ for Li⁺(Cys), 1395 cm⁻¹ for Na⁺(Cys), 1400 cm⁻¹ for K⁺(Cys), 1403 cm⁻¹ for Rb⁺(Cys), and 1393 cm⁻¹ for Cs⁺(Cys). This demonstrates that the [COOH] conformer is not present or abundant for the Li⁺(Cys) and Na⁺(Cys) complexes, but the increase in intensity of this band relative to that of the carbonyl stretch for K⁺(Cys), Rb⁺(Cys), and Cs⁺(Cys) can only be explained by contributions from the [COOH] conformers. This is consistent with theoretical results for these complexes, which indicate that the [COOH] conformers are low-energy structures. Likewise, the umbrella motions of the NH₃ group in the [CO₂⁻] conformers are predicted at 1400 cm⁻¹ for K⁺(Cys), 1389 cm⁻¹ for Rb⁺(Cys), and 1381 cm⁻¹ for Cs⁺(Cys). This red shift is consistent with the IRMPD action spectra for K⁺(Cys), Rb⁺(Cys), and Cs⁺(Cys) and these predicted frequencies lie close to the observed peaks at 1401, 1390, and 1392 cm⁻¹, respectively. Because the bands observed at ~1400 cm⁻¹ are broad in these three spectra, contributions from all three conformations cannot be eliminated.

The experimental IRMPD spectrum for H⁺(Cys) has similarities with those of the lighter alkali metal cation complexes, see Fig. 2. The highest frequency band corresponding to the carbonyl stretch has blue-shifted to 1774 cm⁻¹ compared to 1718–1745 cm⁻¹ for the alkali metal complexes. This is still red shifted compared to the carbonyl stretch of free Cys at 1799 cm⁻¹. Clearly, the hydrogen bond between the protonated amino group and the carbonyl oxygen atom perturbs the carbonyl stretch less than the heavier alkali cations. The other primary distinction in the H⁺(Cys) spectrum is the loss of the band observed near 1000 cm⁻¹ in the M⁺(Cys) spectra. This band corresponds to the NH₂ wagging motion, which is drastically altered in the H⁺(Cys) complex because the NH₃⁺ group hydrogen bonds with both the C-terminal carbonyl and thiol side chain. The intense band at ~1150 cm⁻¹ is observed in all spectra, consistent with the fact that the COH bending motions of the H⁺(Cys) [N,CO] and M⁺(Cys) [N,CO,S] and [COOH] conformers are similar. In contrast, the intense bands near 1400 cm⁻¹ seen in all spectra have no correspondence as they arise from different motions in H⁺(Cys) [N,CO] (NH₃ umbrella) versus those in the M⁺(Cys) conformers.

3.9. Comparison with M⁺(Ser)

The amino acid serine (Ser) differs from cysteine only in the substitution of an oxygen for the sulfur in the side-chain. It is therefore of interest to directly compare results for these two systems. Previously, we have noted that Ser binds to the alkali metal cations more tightly than Cys by a fairly uniform 14 ± 4%, clearly indicating that the hydroxyl side-chain is a better electron donor than the thiol side chain [34,35]. Calculated geometries are generally similar with one important distinction. For Ser, the alkali metal cation prefers to lie in the HOC plane of the side chain (∠MCOH dihedral angles of 179–174° for Li⁺–Rb⁺), i.e., aligned with the dipole moment of the hydroxyl group [34,35]. For Cys, the alkali metal cations have ∠MCSH dihedral angles of 97–110° for Li⁺–Rb⁺, which shows that the metal ions interact with one of the two sp³-like lone pair orbitals on sulfur, i.e., no longer aligned with the local dipole [9].

The IRMPD action spectra of Li⁺(Cys) and Na⁺(Cys) are quite similar to those previously obtained for Li⁺(Ser) and Na⁺(Ser) [13], which is reasonable considering that both involve exclusively similar charge-solvated, tridentate conformations, [N,CO,S] and [N,CO,OH], respectively. As for Cys complexes of K⁺–Cs⁺, IRMPD spectra of the analogous Ser complexes show increasing complex-

ity that are associated primarily with a [COOH] conformation with additional contributions from [CO₂⁻]. In both cases, this is consistent with calculations, which indicate the relative energy of the [COOH] conformation drops considerably from the complexes of Li⁺ to those of Cs⁺, becoming the ground state for Cys (all three levels of theory) and Ser (at both B3LYP and B3P86, where MP2 indicates the [N,CO,OH] structure is still the ground state). The biggest difference in the spectra occurs in the bands associated with the zwitterionic [CO₂⁻] conformer, particularly the asymmetric carboxylate stretch near 1700 cm⁻¹. As noted above, this band appears clearly for K⁺(Cys) and Rb⁺(Cys), whereas it is at best a shoulder for Cs⁺(Cys). In contrast, this band is absent for K⁺(Ser), is very small at best for Rb⁺(Ser), but appears clearly for Cs⁺(Ser). (For the IRMPD spectrum of the related Cs⁺(Thr), this band is again missing despite very similar energetics and conformations [14].) In most respects, the observed trends are consistent with the calculated relative free energies of the [CO₂⁻] conformers, which lie an average of ~9 kJ/mol higher for M⁺(Ser) compared to M⁺(Cys) relative to the [N,CO,S] conformers. (The [COOH] conformers of M⁺(Ser) lie an average of ~4 kJ/mol higher than those of M⁺(Cys) relative to the [N,CO,S] conformers.) Thus, population of the zwitterionic conformer is more favorable in the heavier M⁺(Cys) systems than in those for M⁺(Ser), explaining their observation for K⁺(Cys) and Rb⁺(Cys). As noted above, the failure to observe the asymmetric carboxylate band for the Cs⁺(Cys) system is consistent with its increasing relative energy. Thus, the observation of this band for Cs⁺(Ser) becomes the hardest to explain, especially given its absence for Cs⁺(Thr). As suggested elsewhere, such deviations may be a result of subtle distinctions in the potential-energy landscape connecting the [COOH] and [CO₂⁻] conformers, which are joined by a simple proton motion that is very anharmonic [14].

4. Conclusions

IRMPD action spectra of cationized cysteine in the region of 550–1800 cm⁻¹ have been obtained for complexes with Li⁺, Na⁺, K⁺, Rb⁺, Cs⁺, and H⁺. Comparison of these experimental spectra with IR spectra calculated at the B3LYP/6-311G(d,p) (Li⁺, Na⁺, K⁺ and H⁺ complexes) and B3LYP/HW*/6-311G(d,p) (Rb⁺ and Cs⁺ complexes) levels of theory allow the conformations likely to be present in the experiment to be identified. Comparison of the IRMPD spectra shows that the features observed in the Li⁺(Cys) spectrum are retained for all of the metal cation complexes, but that new spectral features begin to appear for K⁺(Cys) and become very obvious for Cs⁺(Cys). These progressions suggest multiple conformers are present in the IRMPD spectra for the K⁺, Rb⁺, and Cs⁺ complexes.

For Li⁺ and Na⁺ complexes of Cys, the charge-solvated, tridentate structure that binds the metal cation to the amine and carbonyl groups of the amino acid backbone and the sulfur atom of the side chain, [N,CO,S], is the only structure needed to reproduce the IRMPD action spectra, in agreement with the predicted ground state energies of these complexes. The photodissociation spectra of K⁺(Cys), Rb⁺(Cys), and Cs⁺(Cys) have very similar spectral features and are considerably more complex than IRMPD spectra of Li⁺(Cys) and Na⁺(Cys). For these complexes, the bidentate [COOH] conformer, in which the metal cation binds to both oxygens of the carboxylic acid group, is a dominant contributor, although contributions from the tridentate [N,CO,S] conformer remain present. Theoretical results for Rb⁺(Cys) and Cs⁺(Cys) indicate that the bidentate [COOH] conformers are low-energy structures. Contributions from the zwitterionic [CO₂⁻] conformer are also clearly present for K⁺(Cys) and Rb⁺(Cys), but not as obvious for Cs⁺(Cys). For the H⁺(Cys) system, the IRMPD spectrum is characterized by four [N,CO] conformers that differ only in their side-chain orientation and lie within 7 kJ/mol of the tggg⁺ ground state.

Acknowledgments

Financial support was provided by the National Science Foundation, Grants PIRE-0730072, CHE-0748790, CHE-0649039, and CHE-0911191. This work is also part of the research program of FOM, which is financially supported by the Nederlandse Organisatie voor Wetenschappelijk Onderzoek (NWO). The skillful assistance of the FELIX staff is gratefully acknowledged.

Appendix A. Supplementary data

Supplementary data associated with this article can be found, in the online version, at doi:10.1016/j.ijms.2010.04.009.

References

- [1] T. Meinel, S. Blanquet, F. Dardel, *J. Mol. Biol.* 262 (1996) 375.
- [2] O.V. Nemirovskiy, M.L. Gross, *J. Am. Soc. Mass Spectrom.* 9 (1998) 1285.
- [3] O.V. Nemirovskiy, M.L. Gross, *J. Am. Soc. Mass Spectrom.* 7 (1996) 977.
- [4] I. Endo, M. Nojiri, M. Tsujimura, M. Nakasako, S. Nagashima, M. Yohda, M. Odaka, *J. Inorg. Biochem.* 83 (2001) 247.
- [5] A. Miyanaga, S. Fushinobu, K. Ito, T. Wakagi, *Biochem. Biophys. Res. Commun.* 288 (2001) 1169.
- [6] C. Mathe, T.A. Mattioli, O. Horner, M. Lombard, J.-M. Latour, M. Fontecave, V. Nivière, *J. Am. Chem. Soc.* 124 (2002) 4966.
- [7] M. Shindo, K. Irie, H. Fukuda, H. Ohigashi, *Bioorg. Med. Chem.* 11 (2003) 5075.
- [8] N.M. Giles, A.B. Watts, G.I. Giles, F.H. Fry, J.A. Littlechild, C. Jacob, *Chem. Biol.* 10 (2003) 677.
- [9] P.B. Armentrout, E.I. Armentrout, A.A. Clark, T.E. Cooper, E.M.S. Stennett, D.R. Carl, *J. Phys. Chem. B* 114 (2010) 3927.
- [10] C. Kapota, J. Lemaire, P. Maitre, G. Ohanessian, *J. Am. Chem. Soc.* 126 (2004) 1836.
- [11] N.C. Polfer, J. Oomens, R.C. Dunbar, *Phys. Chem. Chem. Phys.* 8 (2006) 2744.
- [12] M.W. Forbes, M.F. Bush, N.C. Polfer, J. Oomens, R.C. Dunbar, E.R. Williams, R.A. Jockusch, *J. Phys. Chem. A* 111 (2007) 11759.
- [13] P.B. Armentrout, M.T. Rodgers, J. Oomens, J.D. Steill, *J. Phys. Chem. A* 112 (2008) 2248.
- [14] M.T. Rodgers, P.B. Armentrout, J. Oomens, J.D. Steill, *J. Phys. Chem. A* 112 (2008) 2258.
- [15] J.T. O'Brien, J.S. Prell, J.D. Steill, J. Oomens, E.R. Williams, *J. Phys. Chem. A* 112 (2008) 10823.
- [16] A.L. Heaton, V.N. Bowman, J. Oomens, J.D. Steill, P.B. Armentrout, *J. Phys. Chem. A* 113 (2009) 5519.
- [17] D.R. Carl, T.E. Cooper, J. Oomens, J.D. Steill, P.B. Armentrout, *Phys. Chem. Chem. Phys.* 12 (2010) 3384.
- [18] J.J. Valle, J.R. Eyler, J. Oomens, D.T. Moore, A.F.G. van der Meer, G. von Helden, G. Meijer, C.L. Hendrickson, A.G. Marschall, G.T. Blakney, *Rev. Sci. Instrum.* 76 (2005) 023103.
- [19] N.C. Polfer, J. Oomens, D.T. Moore, G. von Helden, G. Meijer, R.C. Dunbar, *J. Am. Chem. Soc.* 128 (2006) 517.
- [20] N.C. Polfer, J. Oomens, *Phys. Chem. Chem. Phys.* 9 (2007) 3804.
- [21] D. Oepf, A.F.G. van der Meer, P.W. van Amersfoort, *Infrared Phys. Technol.* 36 (1995) 297.
- [22] A.D. McLean, G.S. Chandler, *J. Chem. Phys.* 72 (1980) 5639.
- [23] R. Krishnan, J.S. Binkley, R. Seeger, J.A. Pople, *J. Chem. Phys.* 72 (1980) 650.
- [24] P.J. Hay, W.R. Wadt, *J. Chem. Phys.* 82 (1985) 299.
- [25] E.D. Glendening, D. Feller, M.A. Thompson, *J. Am. Chem. Soc.* 116 (1994) 10657.
- [26] J.B. Foresman, A.E. Frisch, *Exploring Chemistry with Electronic Structure Methods*, Gaussian, Inc., Pittsburgh, PA, 1996.
- [27] L. Rodriguez-Santiago, M. Sodupe, J. Tortajada, *J. Phys. Chem. A* 105 (2001) 5340.
- [28] R.M. Moision, P.B. Armentrout, *J. Phys. Chem. A* 106 (2002) 10350.
- [29] R.M. Moision, P.B. Armentrout, *Phys. Chem. Chem. Phys.* 6 (2004) 2588.
- [30] J. Bertran, L. Rodriguez-Santiago, M. Sodupe, *J. Phys. Chem. B* 103 (1999) 2310.
- [31] J. Oomens, D.T. Moore, G. Meijer, G. von Helden, *Phys. Chem. Chem. Phys.* 6 (2004) 710.
- [32] W.E. Sinclair, D.W. Pratt, *J. Chem. Phys.* 105 (1996) 7942.
- [33] M.K. Drayß, P.B. Armentrout, J. Oomens, M. Schäfer, *Int. J. Mass. Spectrom.* 297 (2010) 18.
- [34] S.J. Ye, A.A. Clark, P.B. Armentrout, *J. Phys. Chem. B* 112 (2008) 10291.
- [35] V.N. Bowman, A.L. Heaton, P.B. Armentrout, *J. Phys. Chem. B* 114 (2010) 4107.